RAISING THE EFFICIENCY LIMIT OF THE GaAs -BASED INTERMEDIATE BAND SOLAR CELL THROUGH THE IMPLEMENTATION OF A MONOLITHIC TANDEM WITH AN AlGaAs TOP CELL

E. Antolín*, A. Martí, P. G. Linares, I. Ramiro, E. Hernández, and A. Luque
Instituto de Energía Solar–UPM, ETSIT de Madrid, Ciudad Universitaria sn, 28040 Madrid, Spain
*Phone: +34 914533549; FAX: +34 915446341; email: elisa@ies-def.upm.es

ABSTRACT: The high efficiency limit of the intermediate band solar cell (IBSC) corresponds to the case of using as intermediate band (IB) host material a semiconductor with gap in the range of 2 eV. Traditional photovoltaic materials, such as Si and GaAs, are not appropriate to produce IB devices because their gaps are too narrow. To overcome this problem, we propose the implementation of a multi-junction device consisting of an IBSC combined with a single gap cell. We calculate the efficiency limits using the detailed balance model and conclude that they are very high (> 60% under maximum concentration) for any fundamental bandgap from 0.7 to 3.6 eV in the IBSC inserted in the tandem. In particular, the two-terminal tandem of a GaAs-based IBSC current matched to an optimized AlGaAs top cell has an efficiency limit as high as 64%.

Keywords: Fundamentals, Detailed Balance, Intermediate Band, Multi-junction.

1 INTRODUCTION

The efficiency limit of the Intermediate Band Solar Cell (IBSC) is 63.2%[1] according to detailed balance calculations under the 6000K black-body spectrum and maximum sunlight concentration. Such a high efficiency limit has prompted an intensive research on practical ways to implement this novel photovoltaic concept. A great part of the research has been focused on GaAs-based devices, such as the InAs/GaAs quantum dot (QD) IBSC [2, 3]. The development of GaAs IBSCs through the insertion of deep level impurities at high densities is also under study [4].

The choice of GaAs as IB host material to fabricate the first IBSC prototypes is justified by sound practical reasons: it can be synthesized with excellent quality and exhibits dominant radiative recombination, and it is one of the materials that have rendered the most successful results in high concentration PV applications. Also, the InAs/GaAs QD material technology is one of the most developed nanotechnologies to date, mainly because of its application in the production of lasers and LEDs.

However, the gap of GaAs (1.42 eV) is far from being optimum for the implementation of the IBSC concept. The GaAs approach has been regarded as a means to test the operation principles of the IBSC concept (with notable results [2, 5-8]) rather than as a definitive candidate for the fabrication of high-efficiency IBSCs. In this work we will evaluate the potential of implementing a double junction cell (2J) composed of an IBSC and a single gap cell (SGC). The efficiency limit of the SGC/IBSC tandem for any IBSC host semiconductor gap will be presented. This novel IBSC device can allow us to exploit the GaAs-based IBSC technology with the potential to attain really high efficiencies. Therefore, it may constitute a convenient alternative to the use of less known wide-gap materials in a single IBSC, which is also being researched by our group in parallel to this work.

2 THE GaAs-BASED IBSC

Let us first review shortly the IBSC theoretical model and state some nomenclature. Figure 1 (a) shows the band diagram of an ideal IBSC under operation. In the IB material we can define three gaps: the *fundamental gap* or *host material gap* (E_G), between the valence band (VB) and conduction band (CB), and two sub-bandgaps between the IB and CB, and between the VB and IB. The sub-gaps are usually labeled as E_L (the smallest one) and E_H (the largest one). In our calculations we will assume that the IB has a zero width, that is, $E_G = E_H + E_L$.

The high theoretical efficiency limit of this cell relays on its capability of producing extra photocurrent with respect to a single gap solar cell of the same E_G, while preserving a similar output voltage. The first is achieved because sub-bandgap photons can contribute to the photocurrent through a two-step absorption process mediated by the IB (transitions labeled 1 and 2 in Figure 1). The voltage preservation is enabled by the existence of three distinct electronic gasses within the IB material (described by three quasi-Fermi levels) and because the IB material is sandwiched between two emitters that pin the quasi-Fermi levels of holes and electrons at the metal contacts.

It has to be noticed that to attain a high efficiency the spectral splitting among transitions 1, 2 and 3 needs to be optimized. Using a circuital expression, transitions 1 and 2 are series connected (their generation has to be equal for optimal performance) and their generation is parallel connected to that of transition 1. In Fig. 2 we have plotted the limiting efficiency of the IBSC depending on the value of E_G. The absolute limit of 63.2% is achieved for E_G = 1.94 eV. For lower gaps the efficiency sinks because too much light is absorbed in transition 1 and we do not really exploit efficiently the absorption through the IB. These calculations have being made using the original detailed balance model from [1], which assumes the following conditions and idealities: maximum concentration, the solar spectrum modeled as a 6000K black-body, cell temperature set to 300K, non non-radiative recombination or resistive losses, absorptivity = 1, full selectivity between absorption coefficients. The same conditions are maintained for all the calculations presented in the paper.

Coming back to the GaAs case, we see from this plot that the efficiency limit for a 1.4 eV gap is 59%. In fact, the practical situation can be worse, because it is possible that the implementation of an IB in a host material reduces its effective bandgap. In the particular case of the InAs/GaAs QD-IBSC it has been pointed out [9] that the effective gap is reduced to about 1.2 eV. The reason can be seen in Figure 1(b). In this QD material system we have confinement for both electrons and holes. While the electron confined levels are used as the IB, the hole confined levels are nor useful. Since there is almost a continuum of hole states, they can be regarded as an extension of the VB to higher energies. For E_G = 1.2 eV the IBSC efficiency limit 56%.

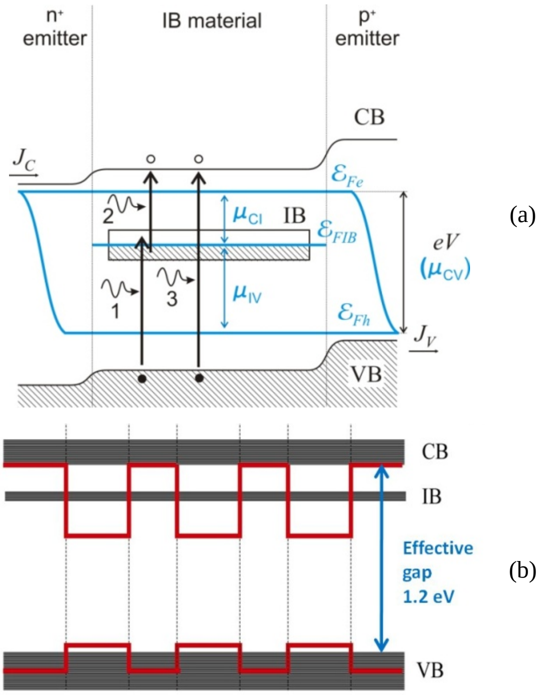

Figure 1. (a) Band diagram of an ideal IBSC under operation conditions, showing the three quasi-Fermi levels (ε_{Fe}, ε_{Fh} and ε_{FIB}) and the corresponding quasi-Fermi level splits (μ_{CI}, μ_{IV} and μ_{CV}). (b) Simplified band diagram of InAs/GaAs QD material, illustrating how the existence of confined hole levels reduces the effective VB-CB gap.

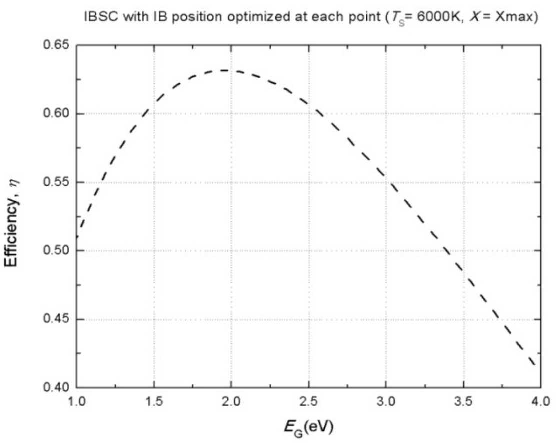

Figure 2. Detailed balance efficiency limit of a single IBSC with optimized IB position, as a function of the fundamental gap E_G.

3 DETAILED BALANCE MODEL FOR THE MULTI-JUNCTION IBSC

We have already presented a detailed balance model for calculating the efficiency limit of a double-junction IBSC (2J-IBSC) [10]. Figure 3 shows a schematic of that device. In principle, the structure is that of a conventional two junction cell where both sub-cells are IBSCs. The bandgaps are labeled following the nomenclature stated before and adding “top” and “bot” for the top and bottom IBSCs, respectively. Besides the conditions listed above, we consider here that a perfect selective reflector is placed between subcells. This is usually included in the detailed balance model of the multijunction solar cell (MJC) (see, for instance, [11]). It means that all photons with energy greater than $E_{L,TOP}$ are reflected back to the top cell, where they can be more efficiently used, while all photons of lower energy pass through to the bottom cell.

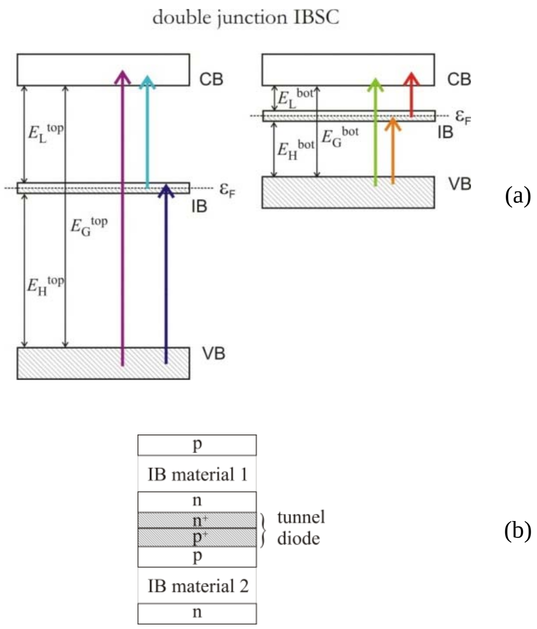

Figure 3. (a) Stack consisting of two IBSCs. (b) two-terminal monolithic stack of two IBSCs connected in series through a tunnel junction.

The absolute efficiency limit of the 2J-IBSC concept is 73.2% when no interconnection between sub-cells is considered (unconstrained case) and 72.7% if series-interconnection (current-matching) is imposed [12]. This limit is comparable to that of a six junction MJC (unconstrained 74.4% and series connected 73.4% [11]). As illustrated in Figure 3 (b), one of the advantages of the 2J-IBSC is that it is possible to implement a two terminal monolithic device using just one tunnel junction instead of the five junctions required for the 6J cell. We consider that this is a promising concept for future applications. However, in the short term, a tandem combining only one IBSC and a SGC is a more feasible device. The results that we present here for this device have being calculated using the same model that in [10, 12], also including the condition of no optical coupling (selective reflector) between sub-cells.

4 EFFICIENCY LIMIT OF THE TANDEM SGC / IBSC AND APPLICATION TO THE GaAs-BASED IBSC

The mixed tandems SGC/IBSC have four different energy thresholds and, thus, should have, in principle, an absolute efficiency limit approaching the absolute efficiency limit of the unconstrained 4J cells. We have evaluated the two possible implementations: with the IBSC as bottom cell and with the IBSC as top cell. The results are shown in Figure 4, red and blue lines respectively. The absolute efficiency limits of these devices are compiled in Table I.

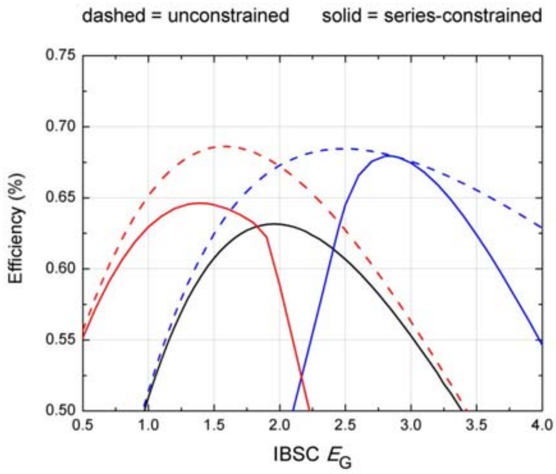

Figure 4. Efficiency limit of the tandem SGC/IBSC considering that the IBSC is the bottom cell (red lines) or that the IBSC is the top cell (blue lines). Dashed repressents the unconstrained and solid the constrained case. The effciency limit of the single IBSC is included for comparison (black line)

Table I. Absolute efficiency limit (η) of different SGC/IBSC and MJC configurations. All gap figures are given in eV.

Tandem top SGC / bottom IBSC, independently connected (this work)				
$E_{G,TOP}$	$E_{G,BOT}$	$E_{L,BOT}$		η (%)
2.39	1.59	0.55		68.6
Tandem top SGC / bottom IBSC, series connected (this work)				
$E_{G,TOP}$	$E_{G,BOT}$	$E_{L,BOT}$		η (%)
1.65	1.39	0.47		64.6
Tandem top IBSC / bottom SGC, independently connected (this work)				
$E_{G,TOP}$	$E_{L,TOP}$	$E_{G,BOT}$		η (%)
2.48	0.96	0.49		68.5
Tandem top IBSC / bottom SGC, series connected (this work)				
$E_{G,TOP}$	$E_{L,TOP}$	$E_{G,BOT}$		η (%)
2.83	1.13	0.52		67.9
4 junctions tandem, independently connected [11]				
$E_{G,1}$	$E_{G,2}$	$E_{G,3}$	$E_{G,4}$	η (%)
2.41	1.61	1.03	0.52	68.7
4 junctions tandem, series connected [11]				
$E_{G,1}$	$E_{G,2}$	$E_{G,3}$	$E_{G,4}$	η (%)
2.02	1.39	0.94	0.51	67.9

The absolute limits of both mixed tandems are very close to the efficiency ceiling of a 4 gap system when they are independently connected, being the configuration with top IBSC marginally better. Both outdo the efficiency of the two-terminal current-matched 4JC. When the sub-cells are series-connected the absolute limit of the tandem with bottom IBSC drops 0.6 points, equaling the current-matched 4JC. But for the top single cell/bottom IBSC system, the series connection produces an efficiency fall of 4 points. The most interesting conclusion from this calculation is that we can have a very high efficiency limit for any fundamental gap of the IBSC from 0.7 to 3.6 eV, even if we impose current matching. Figure 5 shows the optimized $E_{G,TOP}$ and $E_{L,BOT}$ values for the tandem with the IBSC as bottom cell.

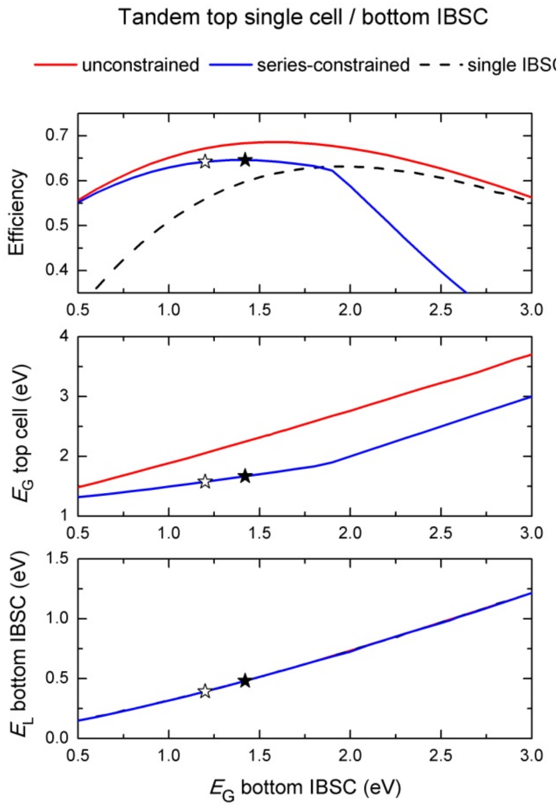

Figure 5. Detailed balance calculations for a 2J-IBSC consisting of a top IBSC and a bottom SGC, in the independently connected case (red lines) and the series-connected case (blue lines). The upper plot represents the maximal efficiency that can be achieved for different values of the fundamental gap E_G of the IBSC. The central and lower plots represent the optimized values of the single gap cell's E_G and the IBSC's E_L (the smaller of the sub-bandgaps) that lead to the efficiencies given in the upper plot. The white (black) star marks the GaAs case with (without) reduction of the effective gap.

The stars in Figure 5 mark the $E_{G,BOT}$ value of GaAs with (white) and without (black) effective gap reduction. In the first case the efficiency limit for the series-connected case is the highest possible (64.6%). With effective gap reduction (E_G = 1.2 eV) the efficiency limit is marginally lower (64.2%). The optimized $E_{G,TOP}$ and

$E_{L,BOT}$ values required for these tandems are indicated in Figure 6. The tandems could be implemented using for the top cell an $Al_xGa_{1-x}As$ alloy with x = 0.19 and 0.12, respectively. With such a low Al content, the gap of AlGaAs is direct and the lattice mismatch to GaAs is negligible. The fabrication of a monolithic AlGaAs/GaAs two-terminal 2JCs is currently a standard technology.

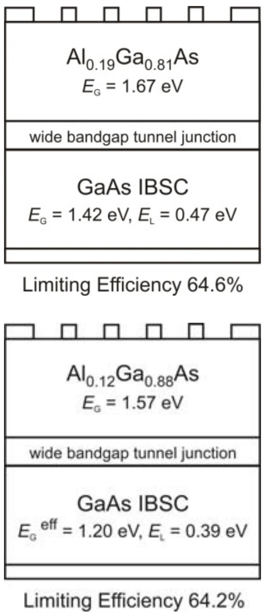

(a)

(b)

Figure 6. Structure of the monolithic series-interconnected AlGaAs/GaAs IBSC tandems proposed in this work: (a) assumes that the GaAs fundamental gap is unaltered by the implentation of the IB, (b) includes a reduction of the GaAs effective gap.

5 CONCLUSIONS

It has been calculated the efficiency limit of a double junction device combining a single gap solar cell and an IBSC. It has been found that it is comparable to that of a four-junction cell (68%) both when the IBSC is used as the top cell or as the bottom cell. This implementation in tandem has an efficiency limit over 60% for any IBSC fundamental gap between 0.7 to 3.6 eV, even under the constraint of current-matching.

An important application of this concept can be the implementation of high efficiency devices using IBSCs of low fundamental gap, such as those based in common photovoltaic materials. In particular it has been found that a GaAs based IBSC can be combined monolithically with an AlGaAs top cell, resulting in an efficiency limit of 64% under current-matching.

ACKNOWLEDGMENTS

This work has been supported by the IBPOWER project funded by the European Commission (Grant Agreement No. 211640), by the Regional Government of Madrid within the project NUMANCIA2 (S2009/ENE-1477), by the Spanish National Research Program within the project Consolider GENESIS-FV (CSD2006-0004) and by MICINN (project NANOGEFES ENE2009-14481-C02-02).

REFERENCES

[1] A. Luque and A. Martí, "Increasing the efficiency of ideal solar cells by photon induced transitions at intermediate levels," *Phys. Rev. Lett.* **78**, pp. 5014–5017, 1997.
[2] A. Luque, A. Martí, N. López, et al., "Experimental analysis of the quasi-Fermi level split in quantum dot intermediate-band solar cells," *Appl. Phys. Lett.* **87**, pp. 083505-3, 2005.
[3] A. Martí, L. Cuadra, and A. Luque, "Quantum dot intermediate band solar cell," in *Conference Record of the 28th IEEE Photovoltaics Specialists Conference*, New York, USA, 2000, pp. 940-943.
[4] A. Martí, E. Antolín, P. G. Linares, et al., "IBPOWER: Intermediate band materials and solar cells for photovoltaics with high efficiency and reduced cost," in *Records of the 34th IEEE Photovoltaic Specialists Conference*, IEEE, Ed., 2009.
[5] A. Martí, E. Antolín, C. R. Stanley, et al., "Production of Photocurrent due to Intermediate-to-Conduction-Band Transitions: A Demonstration of a Key Operating Principle of the Intermediate-Band Solar Cell," *Phys. Rev. Lett.* **97**, p. 247701, 2006.
[6] S. M. Hubbard, C. G. Bailey, C. D. Cress, et al., "Short circuit current enhancement of GaAs solar cells using strain compensated InAs quantum dots " in *Conference record of the 33rd IEEE Photovoltaic Specialists Conference* San Diego, USA: IEEE, 2008.
[7] S. A. Blokhin, A. V. Sakharov, A. M. Nadtochy, et al., "AlGaAs/GaAs photovoltaic cells with InGaAs quantum dot arrays," *Physics and Semiconductor Technique*. **43**, pp. 537-542, 2009.
[8] E. Antolín, A. Martí, P. G. Linares, et al., "Advances in quantum dot intermediate band solar cells," in *35th IEEE Photovoltaics Specialists Conference* Hawaii, 2010.
[9] A. Martí, L. Cuadra, and A. Luque, "Intermediate Band Solar Cells," in *Next Generation Photovoltaics: High Efficiency through Full Spectrum Utilization*, A. Martí and A. Luque, Eds. Bristol: Institute of Physics Publishing, 2003, pp. 140-162.
[10] E. Antolín, A. Martí, and A. Luque, "Energy conversion efficiency limit of series connected intermediate band solar cells," *Proc. of the 21st European Photovoltaic Solar Energy Conference,* pp. 412-415, 2006.
[11] A. S. Brown and M. A. Green, "Detailed balance limit for the series constrained two terminal tandem solar cell," *Physica E*. **14**, pp. 96-100, 2002.
[12] E. Antolín, PhD. Thesis, Insituto de Energía Solar, UPM, Madrid, 2010.